HDA19-mediated deacetylation of histone H3.3 lysine 27 and 36 regulates plant sensitivity to salt stress

Florian Kotnik[a,1], Minoru Ueda[b,c,1], Akihiro Ito[d,e], Junko Ishida[b,c], Satoshi Takahashi[b,c], Katsuyuki Sakai[f], Hiroshi Takagi[f], Julian Seidel[g], Takahiro Abe[b,h], Juergen Eirich[a], Shunji Takahashi[f], Dirk Schwarzer[g], Motoaki Seki[b,c,h,i,2], Iris Finkemeier[a,2]

[a]Institute of Plant Biology and Biotechnology, University of Münster; Münster, 48149, Germany.

[b]Plant Genomic Network Research Team, RIKEN CSRS; Yokohama, 230-004, Japan.

[c]Plant Epigenome Regulation Laboratory, RIKEN CPR; Wako, 351-0198, Japan.

[d]School of Life Sciences, Tokyo University of Pharmacy and Life Sciences; Hachioji, 192-0392, Japan

[e]Drug Discovery Seed Compounds Exploratory Unit, RIKEN CSRS; Wako, 351-0198, Japan.

[f]Natural Product Biosynthesis Research Unit, RIKEN; 351-0198, Japan.

[g]Interfaculty Institute of Biochemistry (IFIB), University of Tübingen, Tübingen, 72076, Germany.

[h]Kihara Institute for Biological Research, Yokohama City University; Yokohama, 244-0813, Japan

[i]Graduate School of Science and Engineering, Saitama University, Saitama, 338-8570, Japan

[1]These authors contributed equally to this work

[2]Corresponding author. Email: motoaki.seki@riken.jp (M.S.); iris.finkemeier@uni-muenster.de (I.F.)

Author Contributions: M.U., M.S., D.S., and I.F. designed research; F.K., M.U., A.I., S. T., K.S., H.T., S.T., J.E., J.I., J.S., and T.A. performed research; F.K. and M.U. analyzed data; and F.K., M.U., M.S., and I.F. wrote the paper.

Competing Interest Statement: The authors declare that they have no competing interests.

Data and materials availability: Mass spectrometry proteomics data have been deposited at the ProteomeXchange Consortium (https://proteomecentral.proteomexchange.org/ui) via the JPOSTDB partner repository (https://repository.jpostdb.org/) with the identifiers JPST004010 and PXD067353.

Gene identifiers and sequence information can be found in The Arabidopsis Information Resource-TAIR database (www.arabidopsis.org) under the following accession numbers: HDA19 (AT4G38130), HTR4 (AT4G40030), HTR5 (AT4G40040), HTR8 (AT5G10980), LEA7 (AT1G52690), LEA29 (AT3G15670), RAB18 (AT5G66400). Plasmids and seeds are available from M.S. upon reasonable request.

Classification: Biological Sciences, Plant Biology

Keywords: Histone deacetylase, histone acetylation, salinity stress response, Arabidopsis

This PDF file includes:

Main Text
Figures 1 to 6

Abstract

Plants survive extreme environments through rapid chromatin reprogramming, yet the epigenetic marks that confer stress resilience remain poorly understood. Histone deacetylase HDA19 is a key epigenetic regulator in Arabidopsis, and *hda19*-deficient mutants display tolerance to multiple abiotic stresses, including drought, heat, and salinity. Using lysine acetylome profiling, we identified a non-canonical K27/K36 di-acetylation mark on histone H3.3, among nine H3 variants, as a specific substrate of HDA19. Under salinity stress, this mark decreased in wild-type plants but increased in *hda19* mutants, while other known H3 modifications were similarly affected in both genotypes. Mimicking constitutive di-acetylation of H3.3 K27/K36 through lysine-to-glutamine substitutions promoted accumulation of stress-responsive late embryogenesis abundant (LEA) proteins and conferred salinity tolerance in seedlings, phenocopying *hda19* mutants. Furthermore, generating the *lea7-1/lea29-1/rab18-1* triple mutant abolished *hda19*-dependent salinity tolerance, confirming the LEA proteins' role downstream of HDA19. Our findings demonstrate that H3.3 K27/K36 di-acetylation, modulated by HDA19, drives LEA protein accumulation and enables plants to withstand environmental stress, revealing a previously unknown core mechanism of plant stress resilience.

Significance statement

Histone acetylation is crucial for regulating chromatin states and transcription, yet the specific histone codes controlled by histone deacetylases and acetyltransferases during plant stress acclimation remain unclear. Arabidopsis mutants lacking histone deacetylase 19 show enhanced tolerance to drought, heat, and salinity. Using acetylome profiling and genetic analyses, we identify a previously unknown di-acetylation of histone H3.3 at lysines 27 and 36 as a key epigenetic switch activating late embryogenesis abundant proteins essential for salt tolerance in seedlings. This discovery reveals a novel mechanism linking histone H3.3 K27/K36 di-acetylation to stress-resilient protein accumulation, offering new insights into epigenetic control of plant stress responses and informing strategies to improve crop resilience under climate change.

Main Text

Introduction

Abiotic stressors like salt stress pose significant threats to crop yields. Hence, the elucidation of the molecular mechanisms underlying plant stress responses is crucial for developing resilient crops. Histone deacetylase 19 (HDA19), also known as HDA1 or HD1, plays a key role in regulating gene expression during plant development and in response to stress (1-4). However, the mode of action of HDA19 in driving epigenetic regulatory machinery in response to stress remains unclear.

Within the nucleus of eukaryotic cells, core histone proteins (H2A, H2B, H3 and H4) wrap DNA into higher order structures called nucleosomes, enabling sophisticated regulation of nuclear gene expression and protecting DNA from physical damage. Multiple post-translational modifications (PTMs) can occur on the N-terminal tails of histones and play a crucial role in regulating chromatin structure and, consequently, gene expression. The most important histone PTMs include lysine acetylation, various other acylations, lysine and arginine methylation, lysine ubiquitination as well as serine and threonine phosphorylation. Based on the interplay of these modifications, which are essential for chromatin structure and gene activity regulation, a histone

code theory was proposed (5-8). Previous studies have established a positive correlation between levels of lysine acetylation at N-terminal histone H3 sites and active gene expression (9, 10). The interplay between histone acetyltransferases (HATs) and HDACs acts as a dynamic regulatory mechanism, with these enzymes functioning as writer and eraser proteins that modulate the acetylation status at distinct histone sites (11). Reader proteins, including bromodomain-containing proteins, specifically recognize acetylated sites and recruit transcriptional complexes to target genes, thereby determining their activation state. Notably, various histone H3 variants, characterized by subtle alterations in their tail domains, have been shown to play unique roles in regulating gene expression and plant development. For instance, histone H3.3 is predominantly associated with transcriptionally active regions during Arabidopsis development, whereas the H3.1 variant is more commonly found in inactive heterochromatic regions (12).

In Arabidopsis, the HDAC family comprises three classes: HDA1/RPD3-type, sirtuin, and HD-tuin subfamilies, consisting of 18 genes. Each HDAC has diversified its function and plays pivotal roles in various biological processes (13). As a member of the RPD3-type subfamily of class I histone deacetylases, HDA19, together with HDA6 and HDA9, is involved in the epigenetic regulation of gene expression. HDA19 deficiency leads to a high tolerance towards salt, dehydration, and heat stresses with slower development and reduced fertility in Arabidopsis Col-0 and rice (13-16). Despite growing recognition of the importance of HDA19 and its homologue in rice in stress responses (17), its substrates remain unclear. Most studies have focused on its role in regulating specific histone marks, such as H3K9ac, H3K9K14ac, and H3K9K18ac, which are commonly conserved among eukaryotes including yeast, plants, and mammals (18).

Recent mass spectrometry-based (MS) lysine acetylome studies in plants and mammalian cell culture using the RPD3-class inhibitor apicidin have comprehensively revealed significant changes in the nuclear acetylome when the activity of this class of deacetylases is modulated, affecting both histone and non-histone proteins (19, 20). The diversification of primary structures of plant histones (H2A; 6 variants and 13 genes, H2B; 11 variants and 11 genes, H3; 9 variants and 15 genes in Arabidopsis), except for H4 (21), and the emergence of plant specific accessory proteins like angiosperm-specific HDA19-interacting homologous proteins (HDPIs) (22), highlight the need for a comprehensive dissection of *hda19* mutants to uncover acetylation marks through which HDA19 dominantly regulates stress responses. In this work, we found that di-acetylation of H3.3 at K27/K36 mediates salt tolerance, whereas the absence of HDA19 has only a minor effect on canonical acetylation marks, including H3K9ac, H3K9K14ac, and H3K9K18ac. Furthermore, lysine-to-glutamine (K/Q) substitutions, which mimic the acetylated states at this novel di-acetylation site, induce the expression of late embryogenesis abundant (LEA) proteins, thereby conferring salt stress tolerance comparable to that observed in *hda19* mutants.

Results

***Rfhda19*, a novel *hda19* allele with reverted fertility and maintained stress tolerance.** Our previous work showed that the *hda19-3* mutant, which is deficient in HDA19, exhibits a severe defective phenotype in reproductive organ-formation and fertility, as well as a salt and drought stress tolerance phenotype. In this study, we aim to identify the *in vivo* HDA19 substrates by mass spectrometry-based acetylome profiling to elucidate the mechanism by which *hda19* mutants acquire their tolerance. The slow growth of the *hda19-3* mutant made it challenging to directly compare them with Col-0 wild-type (WT) plants. To address this issue, we screened for additional *hda19* mutant alleles that retained their stress tolerance but had a less severe growth defect. For this screen we used the *hda19-7* line, which was selected from a CRISPR-Cas mediated genome-editing experiment as described previously (16). *hda19-7* contains an additional G insertion 79 nucleotides downstream of the start codon within *HDA19* coding sequence. Among the progeny of this line, we identified a revertant in fertility, designated *Rfhda19* for this reason. This *Rfhda19* mutant contains an additional insertion of plasmid-like foreign DNA into the genomic region around the translational initiation site of HDA19, resulting in the deletion of 57 nucleotides from the HDA19 coding sequence, which leads to a modified N-terminus of the protein (*SI Appendix*, Fig. S1*A*).

136 *Rfhda19* retains similar stress resistance to *hda19-3* and exhibits partial recovery to semi-fertility
137 from almost sterile phenotypes, enabling better growth and allowing for a more suitable comparison
138 to WT plants (Fig. 1*A*, *SI Appendix*, Fig. S1, *B* to *D,* Fig. S2*A*). To confirm that the phenotype is
139 caused by the lack of active HDA19, the genomic DNA encompassing the coding sequence and
140 proximal regulatory elements of *HDA19* was introduced into *Rfhda19*, and the resultant T_3 plants
141 displayed decreased tolerance to salinity stress as WT plants (*SI Appendix*, Fig. S1 *E* and *F*). To
142 determine if the *Rfhda19* line also lacks an active HDA19 enzyme, we performed a pull-down
143 analysis using the HDAC-trap mini-AsuHd, which enriches catalytically active HDACs by
144 hydroxamic acid grafted onto a lysine-like scaffold (23). While HDA19 was highly enriched on mini-
145 AsuHd from WT extracts, it was absent in *Rfhda19* mutants (*SI Appendix*, Fig. S3 and Dataset S1)
146 due to its impaired activity.

147 **Histone H3.3 and seed-specific proteins are hyperacetylated *in hda19*.** To identify the *in vivo*
148 protein substrates of HDA19, we analyzed the proteomes and acetylomes of five-day-old
149 Arabidopsis seedlings from the two different lines lacking HDA19 (*hda19-3* and *Rfhda19)* compared
150 to WT plants using a quantitative liquid chromatography mass spectrometry-based (LC-MS)
151 proteomic approach. In total, 4989 and 4428 protein groups were quantified in at least two biological
152 replicates in the *Rfhda19* and *hda19-3* versus WT comparisons, respectively. Moreover, 3726 and
153 3318 lysine acetylation (acK) sites were quantified on 1669 and 1465 unique protein groups,
154 respectively (*SI Appendix*, Fig. S4 and S5, Dataset S2 and S3). The majority of protein groups and
155 1912 lysine acetylation (acK) sites were common to both *hda19* deficient lines in these datasets
156 (*SI Appendix*, Fig. S6). To reveal whether similar changes in protein and acK site abundance
157 changes occur in both *hda19* mutant lines, we directly compared the regulation patterns between
158 the two lines. Scatter plots illustrate a high degree of similarity between the two *hda19* mutants
159 relative to WT, with 44 protein groups and 63 acK sites on 36 protein groups exhibiting strong
160 increases in abundance in both lines ($\log_2$ FC > 1) (Fig. 1, *B* and *C*). Given this high degree of
161 correlation of the proteome response in both lines, we combined them into a single group (*hda19*)
162 and considered protein groups and acK sites quantified in six out of eight replicates for further
163 statistical analysis. This combined analysis revealed 94 acK sites on 49 protein groups with
164 significantly and more than two-fold increased hyperacetylation ($\log_2$ FC > 1, FDR < 5%) (Fig. 2, *A*
165 and *B*, Dataset S4). The strongest increase in lysine acetylation (>16-fold) was observed for the
166 seed storage protein CRUCIFERIN 4 (CRU4) and LEA29 (*SI Appendix*, Fig. S7). Only 11 of the 49
167 hyperacetylated proteins (AHL14, Ankyrin repeat family protein (AT2G26210), DNA-binding
168 storekeeper protein-related transcriptional regulator (AT4G00390), H3.3, LEA7, LEA25, LEA29,
169 MAC7, PARP3, PWO1, SCS2B) are known to localize to the nucleus, and one (RAB18) to the
170 nucleus and plasma membrane, according to SUBA5 (Fig. 2*C*). A sequence logo generated from
171 the 94 hyperacetylated sites revealed a putative substrate motif for HDA19, characterized by lysine
172 residues at positions -13, -2, and +11, and alanine residues at positions -3 and +1, and aspartic
173 acid at position -1 surrounding the actual acetylation site (Fig. 2*D*). Functional enrichment analysis
174 of the hyperacetylated proteins showed that the GO Component term "protein storage vacuole",
175 the GO Function term "nutrient reservoir activity", and the UniProt Keyword "seed storage protein"
176 were the three terms most enriched terms (Fig. 2*E*). Comparison of proteome and acK site
177 abundance changes revealed a high correlation, with 24 protein groups exhibiting similar increases
178 in acetylation and protein abundance in *hda19* compared to WT (Fig. 2*F*). However, 24 acK sites
179 on 19 proteins showed an at least 2-fold stronger increase in lysine acetylation than in protein
180 abundance. Among these 19 proteins, the histone protein H3.3 with two acetylation sites (K27 and
181 K36) and multiple LEA proteins with various acK sites (LEA25 K300; LEA29 K38, K82, K111;
182 LEA48 K153; RAB18/LEA51 K180) were identified.

183 **Histone H3K27/K36 di-acetylation is indispensable for salinity tolerance.** Gene expression is
184 heavily influenced by histone modifications, with even minor variations in histone sequences giving
185 rise to distinct regulatory functions. In Arabidopsis, 50 genes encode 37 different histone proteins
186 (24). We quantified 32 of those histone proteins at either the protein or acetylation level (Dataset
187 S4). Due to the high lysine content of histone tails, tryptic peptides often carry more than one acK

site. This is particularly important, as H3.3 hyperacetylation was only observed on peptides carrying di-acetylation at both K27 and K36, while peptides showing mono-acetylation only at K36 were slightly downregulated (Fig. 3*A*). Since the differences in amino acid sequences between the histone variants are relatively small, distinguishing between them is not always possible, especially for acK sites where the corresponding amino acid changes may not reside on the same tryptic peptide. In the case of H3.3, a single amino acid exchange from alanine to threonine between H3.1 and H3.3 can be found at position 31 (24), which is distinguishable in the MS/MS spectra of the di-acetylated peptide (Fig. 3*B*). H3.3 is often enriched at euchromatin regions and associated with active gene expression, whereas H3.1 is enriched in heterochromatin and associated with gene silencing (25). Both acetylome and immunoblotting analyses detected a significant increase in di-acetylation levels of lysines (K) 27 and 36 of histone H3.3 (H3.3K27/K36ac) in *hda19* compared to WT plants, although this increase was less pronounced in *Rfhda19* (Fig. 2*F*, Fig. 3, *A* and *C*). The difference between *hda19-3* and *Rfhda19* may be attributed to the fact that a truncated, non-active HDA19 protein might be generated in *Rfhda19*, although this was not detectable by LC-MS/MS analysis. Additionally, the difference could be caused by the slightly enhanced developmental speed of *Rfhda19* compared to *hda19*-3, particularly given that H3.3 enrichment patterns change during early development (26). Plants treated with trichostatin A (TSA), a pan-HDAC inhibitor, showed a 2-fold increase of acetylation at H3.3K27/K36ac compared to control conditions in the immunoblot analysis (Fig. 3*C*). Similarly, a previous MS-based analysis of apicidin treated plants showed a nearly 6-fold increase in di-acetylation of H3.3K27/K36ac (19). Higher acetylation levels of K27/K36 after inhibitor treatments may be explained by additional inhibition of HDA6, which is thought to work redundantly with HDA19 (27). In contrast to *Rfhda19* treated with salt, WT plants showed slightly decreased di-acetylation of K27 and K26 under the same conditions (Fig. 3*A*). This is consistent with a previously observed up-regulation of HDA19 activity upon salt stress in WT plants (28). Here we detected increased lysine acetylation on H3.3 only in the absence of HDA19 (Fig. 3*A*), indicating that HDA19 can distinguish between histone variants to regulate gene expression.

To confirm the role of H3.3K27/K36ac in response to salinity stress, we introduced two K to Q mutations at the 27 and 36 sites of histone HTR5, a variant of H3.3 in Arabidopsis. The replacement of lysine residues with glutamine (K→Q) is considered to mimic the acetylation mark due to the permanent abolishment of the positive charge (29). Three different genes, HTR4/5/8, encode H3.3 in Arabidopsis (24). Expression of HTR5:FLAG complemented the *htr4/5/8* mutant derived from *htr4/5*(-/-) *htr8*(+/-) progeny (*SI Appendix*, Fig. S8), indicating that FLAG-tagged HTR5 is functional, whereas constitutive expression of K27Q/K36Q in all three H3.3 variants appears lethal in Arabidopsis, as HTR5K27Q/K36Q:FLAG was detected only in an *htr4/5* background but not in *htr4/5/8* progeny. Plants expressing HTR5K27Q/K36Q:FLAG under the control of the gene-specific promoter and terminator showed salinity stress tolerance (Fig. 3, *D* and *E, SI Appendix*, Fig. S2*B*). These data indicate that H3.3K27/K36ac regulates the response to salinity stress in Arabidopsis.

Identification of HDA19 interaction partners in Arabidopsis seedlings. Previous studies have identified several proteins that interact with HDA19 in chromatin-modifying complexes. To further investigate the interactions of HDA19, we performed a quantitative pull-down analysis of MycHDA19 expressed in *hda19-6* seedlings compared to WT plants via LC-MS. In total, 203 protein groups were quantified in at least two out of four replicates, and 22 of those protein groups were significantly enriched ($\log_2$ fold-change > 1 and adjusted p-values (FDR) < 0.05) in MycHDA19 compared to WT, including HDA19 itself (Fig. 4, Dataset S5). Among these 22 proteins, nine localize to the nucleus and five to the cytosol, suggesting that HDA19 might also function in more than one compartment. We detected multiple members of the known HDA19-SIN3 complex, including HISTONE DEACETYLASE COMPLEX 1 (HDC1), MSI1, SIN3-like (SNL) proteins 1-6 (14, 30-32). Recently, three new angiosperm specific members of the HDA19-SIN3 complex called HDIPs were identified (22). HDIP3 co-purified with MycHDA19 in this study, along with several previously unreported proteins (Fig. 4), including the small GTP-binding protein RAN1,

which regulates nuclear-cytoplasmic transport (33), four ribosomal proteins, and the dynamin-related protein 2 family protein important for gametophyte development and biotic stress resistance (34, 35). These HDA19 interacting proteins are likely to play a crucial role in regulating stress responses through the modification of H3.3K27/K36ac.

Requirement of LEA proteins in enhancing salinity stress tolerance in *hda19* mutants. LEA proteins play crucial roles in protecting plants against environmental stresses, such as desiccation, drought and salinity. Despite their importance, the regulation of LEA proteins is not yet fully understood. In total, 22 out of 51 LEA proteins were quantified at either the protein or acK level (Fig. 5*A*). These proteins belong to different subfamilies, including LEA_1, LEA_2, LEA_3, LEA_4, dehydrins, and PvLEA18. LEA_4 family is the largest of these, comprising 19 LEA proteins, of which nine were found in this dataset (36). Here we report that the protein abundance of 11 LEA proteins and 33 acK sites of seven of these proteins were strongly upregulated in *hda19* mutants (Dataset S4). The strongest induction was primarily observed for the LEA_4 family members, with many proteins showing significant increases in both protein and acK site abundance. The highest increase was observed for LEA29 acK sites K38, K82, and K111, which showed an over 11-fold increase in the *hda19* mutants compared to WT plants (Dataset S4). LEA7, a paralog of LEA29 with preserved nucleotide similarity, was duplicated as a result of a whole-genome duplication event (36) and also exhibited increased protein abundance and acK levels in *hda19* mutants. In addition to the LEA_4 family proteins, the acetylation of the dehydrin RAB18/LEA51 was also strongly increased at K180 (Fig. 5*A*). Both LEA7 and LEA29 have been reported to be induced under salt and osmotic stress, and during treatment with the plant hormone abscisic acid (ABA) (37). RAB18 is also induced in response to salinity, ABA, and other environmental stresses (36, 38). To test whether these LEA proteins contribute to the enhanced salinity tolerance of *hda19* mutants, we generated higher-order mutants. The quadruple *lea7-1/lea29-1/rab18-1/Rfhda19* mutants showed markedly reduced tolerance to 125 mM NaCl, with a survival rate of 36.7% (Fig. 5*B*), compared with 73.3% in *Rfhda19* mutants (Fig. 5*B, SI Appendix*, Fig. S2*C*). To determine whether the mRNA expression of LEA7, LEA29, and RAB18 is regulated by H3.3K27/K36ac, we analyzed mRNA levels in plants expressing HTR5 K27Q/K36Q:FLAG. Their transcript abundance was significantly elevated in these plants relative to WT, *htr4/5* mutant backgrounds, as well as in plants expressing HTR5:FLAG (Fig. 5*C*). Chromatin immunoprecipitation (ChIP)-qPCR detected the localization of both HTR5:FLAG and HTR5 K27Q/K36Q:FLAG at *LEA7*, *LEA29*, and *RAB18* genes (Fig. 5 *D* and *E*). Together, these results indicate that H3.3 is enriched at different *LEA* genes but that only H3.3. di-acetylation at K27 and K36 results in induced LEA gene expression. The analysis of the quadruple mutant revealed that LEA7, LEA29, and RAB18 proteins promote salinity tolerance in *hda19* mutants (Fig. 6).

Discussion

Our study revealed that the di-acetylation site H3.3K27/K36ac is a critical epigenetic mark regulated by HDA19, which plays a key role in salinity stress tolerance in Arabidopsis. Hyperacetylation of these amino acids was found to drive the up-regulation of LEA proteins at both the transcript and protein levels in *hda19* mutants, thereby conferring salt stress tolerance.

Histone modifications represent a "histone code" that recruits transcriptional regulators to activate or repress mRNA synthesis. These histone codes are regulated by writers (catalyzing modifications), erasers (removing modifications), and reader (recognizing modifications) proteins (39, 40). Elucidating the interactors of each histone code is essential for understanding their role in the respective biological processes. The acetyltransferase GCN5 may play an antagonistic role to HDA19 at H3.3K27/K36ac sites, as it has been shown to acetylate H3K27 and K36 in Arabidopsis to activate transcription in euchromatin (41-43). The opposing photomorphogenesis phenotypes observed in *gcn5* and *hda19* mutants were absent in a double mutant (43). Furthermore, HDA19 may influence the activity of the SAGA complex, as evidenced by the hyperacetylation of its subunits TAF5 and SCS2B in *hda19* mutants. In addition to HDA19, the Arabidopsis genome encodes for three other class I HDACs (HDA6, HDA7, and HDA9) (13), although HDA7 is

291 considered to be a pseudogene due to the of loss of the Zn^{2+} binding site in the catalytic pocket
292 (44). HDA9, another class I HDAC, is also thought to mediate H3K27 deacetylation (45). The mono-
293 deacetylation of H3K27ac seems to be redundantly regulated by multiple enzymes. In contrast to
294 *hda19*, *hdc1* mutants are sensitive towards salt stress in comparison to WT plants (46). In *hdc1*
295 H3K9K14ac correlates with the expression of LEA14 and RAB18 under salt stress. However, a
296 *lea14* mutant showed an increased but not a decreased tolerance towards salt stress (46), and
297 thus cannot be responsible for the salt-tolerance observed in the *hda19* mutants. Hence, the
298 function of *hda19* in the salt response is different to that of *hdc1*, and further characterization of
299 novel HDA19 substrates and interacting proteins will enhance our understanding of how plants
300 regulate stress responses through H3.3K27/K36ac di-acetylation.

301 In addition to H3.3K27/K36, we identified further 48 putative substrate proteins with a
302 consensus acetylation motif for HDA19, including 38 proteins that are not known to localize to the
303 nucleus (Figs. 1 and 2). This raises questions about the subcellular localization of HDA19 and its
304 substrates that require further investigation. Previously, HDA19 was reported to be exclusively
305 localized to the nucleus (47); however maize RPD3-type HDACs have also been reported to have
306 both a nuclear and cytoplasmic localization (48), and a significant proportion of Arabidopsis HDA9
307 was also found in the cytoplasm (49). Furthermore, human class I HDAC3 has been shown to
308 reside in both the nucleus and cytosol, owing to its possession of a nuclear export signal (50).
309 Additionally, human HDAC1-3 have been detected in the endoplasmic reticulum, where they play
310 a role in modulating the unfolded protein response (51).

311 We demonstrate that three LEA proteins, which are ABA-responsive genes (36), are
312 essential for the salt tolerance conferred by HDA19 deficiency (Fig. 5, *B*). The mapping of ChIP-
313 seq data deposited by Liu et al (21), shows that HDA19 localizes at *LEA29* and *RAB18* genes (*SI*
314 *Appendix*, Fig. S9). Combined with the ChIP-qPCR analysis of H3.3K27Q/K36Q mutants
315 performed in this study (Fig. 5, *E*), our results suggest that HDA19 directly controls the mRNA
316 abundance of *LEA* genes through the acetylation status of histone H3.3 K27/K36 in response to
317 salinity stress (Fig. 6).

318 LEA proteins were described to accumulate during seed maturation, where they help
319 protect cells during seed desiccation (52, 53). Expression of LEA proteins has been detected in
320 non-plant taxa, various plant organs, and under different stress conditions, suggesting a broader
321 role for LEA proteins in stress responses (36, 54, 55). The strong hyperacetylation of LEA proteins,
322 particularly LEA29, implies a more direct role for HDA19 in regulation LEA proteins. Although no
323 enzymatic functions have been reported for LEA proteins to date, multiple models have been
324 proposed to explain their involvement in stress tolerance. These models include binding and
325 potentially stabilizing membranes or binding directly to proteins to prevent aggregation in a
326 chaperone-like manner (56, 57). Additionally, a molecular shield function has been suggested,
327 where LEA proteins contribute to molecular crowding, preventing molecule collisions (58). LEA
328 proteins, such as LEA7 and LEA29, are highly disordered in solution but form a high number of α-
329 helices during drying (59, 60). LEA29 has been shown to form homodimers and heterodimers with
330 LEA7 in tobacco leaves (61). The secondary structure formation of LEA7 appears to be partly
331 dependent on the presence of membranes, although a stabilizing effect on liposomes during drying
332 was not observed (60, 62). A protective effect of LEA7 on the activity of lactate dehydrogenase
333 during freezing and drying was observed (62). Therefore, the accumulation and acetylation of
334 LEA29, LEA7, and RAB18 may contribute to the protection of membranes and proteins under
335 stress conditions. The involvement of LEA proteins in stress responses is well established, not only
336 in Arabidopsis but also in crops (63-65). Elucidating the mode of action of these acetylated LEA
337 proteins in the future will provide valuable insights into tolerance of salinity stress in plants.

338 Overall, our findings suggest that ABA signaling is the key pathway controlled by HDA19
339 via the regulation of histone H3.3 K27/K36 di-acetylation in response to salinity stress. Recently,
340 angiosperm-specific HDA19-interacting proteins (HDPIs) have been identified (22), and were also
341 found in our HDA19 seedling interactome (Fig. 4), along with other new interacting proteins.
342 Although HDACs are highly conserved among eukaryotes, the study of plant-specific HDA19-

343 interacting proteins, such as HDPIs, will provide further insights into the molecular mechanisms of
344 ABA signaling regulation through H3.3 K27/K36ac.
345 In summary, our study identifies the histone H3.3 di-acetylation site K27/K36 as a key
346 mediator of salinity stress tolerance, regulated by HDA19. Further characterization and
347 identification of the coordinators of H3.3 K27/K36ac will reveal specific targets for manipulating
348 stress responses, as HDACs represent a promising target for chemical intervention in various
349 biological processes.

350 **Materials and Methods**
351 Detailed description of plant growth conditions, the preparation of transformants, immunoblotting,
352 RT–qPCR, ChIP-qPCR, and methods used for data analysis can be found at *SI Appendix*, *Materials*
353 *and Methods*.

354 **Plant material.** *Arabidopsis thaliana* (L.) Heynh. (Columbia: Col-0 as wild-type accession in this
355 study), *hda19-3* (66); SALK_139445, *htr4htr5-1* (67); SALK_042781, *htr8-3* (67); SALK_087850,
356 *lea7-1* (68); SALK_205942 (Col-0), *hda19-7* [the mutant has an additional base 79G inserted in the
357 *HDA19* gene and is a novel allele is resulting from a progeny of genome-edited Col-0 plants using
358 the same guide RNA as reported in our previous study (16)], Reverted fertility in *hda19-7* (*Rfhda19*)
359 (see for details *SI Appendix*, Fig. S1*A*), *lea29-1* (in 104T, a genome-edited allele) (*SI Appendix*,
360 Fig. S10*A*) and *rab18-1* (in 223A, a genome-edited allele) (*SI Appendix*, Fig. S10*B*) and were used
361 in the course of this study.

362 **Evaluation of salinity tolerance.** When plants were 5 days old (counted from seed germination),
363 20 µL or 25 µL of 5 M NaCl were added to each well, yielding final concentrations of 100 mM or
364 125 mM NaCl per well, respectively, while control plants received no salt. Percent survival was
365 assessed five days later using three biological replicates, each containing 15 plants. Plants with
366 green true leaves were scored as survivors. Survival rates were statistically analyzed by a one-way
367 ANOVA in the GraphPad Prism version 10. 2. 3 for Windows (GraphPad Software).

368 **Primary antibodies for Immunoblotting and ChIP-qPCR.** Primary antibody dilutions were as
369 follows: H3.3 (HTR4/HTR5/HTR8) K27/K36ac, 1: 500 (polyclonal antibody raised against
370 H3.3K27acK36ac in this study); H3, 1:2,000 (polyclonal, Abcam, Cambridge, MA, 1791); and Myc-
371 tag, 1:1,000 (monoclonal, MBL, Japan M185-3L). Synthetic peptides
372 [CKAARKAcSAPTTGGVKAcKP] were used as antigen to produce polyclonal antibodies against
373 H3.3K27/K36ac (Scrum, Tokyo, Japan).

374 **Enrichment of active HDACs using AsuHd probes.** Plant material was homogenized and
375 suspended in extraction buffer (EB) containing 50 mM HEPES (pH 7.5), 150 mM NaCl, 10% [v/v]
376 glycerol, 5 mM ascorbate, 0.25% [v/v] Triton X-100, and cOmplete™ EDTA-free Protease Inhibitor
377 Cocktail (Roche). Extracts were incubated at 4 °C for 1 h with constant agitation, and cell debris
378 was pelleted by centrifugation at 18,000 x *g* for 25 min at 4 °C. Protein concentrations in the
379 supernatants were determined using the Pierce 660 nm Protein Assay (Thermo Fisher Scientific).
380 Resins with mini-AsuHd (HDAC trap) and mini-Lys peptide (control) probes (23), were equilibrated
381 3x with 600 µL wash buffer (WB) (50 mM Hepes pH 7.5, 150 mM NaCl, 10% [v/v] glycerol, 5 mM
382 ascorbate). Equal amounts of each sample (2.5 mg) were incubated overnight at 4 °C with 10 µL
383 of both mini-AsuHD and mini-Lys beads under constant agitation. Beads were transferred onto a
384 micro-centrifugal filter system (amchro GmbH) and washed 5x with 250 µL WB. An on-bead trypsin
385 digestion was performed as described previously (28). Peptides were desalted using C18 Stage
386 tips (69) prior LC-MS/MS analysis.

387 **Myc pulldown.** Plant material was homogenized and suspended in EB buffer as described above.
388 EZview™ Red Anti-c-Myc Affinity Gel (Merck Millipore, Darmstadt, Germany) was equilibrated 3x
389 with WB (50 mM Tris pH 7.5, 150 mM NaCl, 10% [v/v] glycerol, 2 mM EDTA). Protein extracts were
390 incubated on beads over-night at 4 °C with constant agitation. Beads were collected by slow
391 centrifugation (500 x *g*) at 4 °C and washed 3x with 1 mL WB for 5 min with constant agitation.
392 Proteins were eluted two times with 30 µL 0.1% (v/v) TFA for 5 min and collected by gentle
393 centrifugation. An in-solution trypsin digestion was performed as described previously. For total

proteome analysis, peptides from input samples were prepared using small-scale filter-aided sample preparation (FASP) as described previously (70).

Quantitative proteomics and lysine acetylome. Proteins were extracted from plant material under denaturing conditions as described previously (71). DTT was replaced with tris(2-carboxyethyl)phosphine (TCEP). Proteins were processed using single-pot, solid-phase-enhanced sample preparation (SP3) (72). After the tryptic digest, peptides were labeled using tandem mass tags (TMT) (73). TMT10plex™ (Thermo Fisher Scientific) reagents were used. Samples were randomized within each TMT set. Each channel was assigned to one genotype or treatment, or a pool of all samples for normalization purposes. Peptides were resuspended in TBS buffer (50 mM Tris–HCl, 150 mM NaCl, pH 7.6). A more than 98% labeling efficiency was confirmed by LC-MS/MS analysis and samples were pooled afterwards. 30 µg of pooled peptides was stored for whole proteome analysis. Lysine-acetylated peptides were enriched using PTMScan® Acetyl-Lysine Motif [Ac-K] Immunoaffinity Beads (Cell Signaling Technology) as described previously (71). All total proteome and acetylome samples were desalted using SDB-RPS Stage tips (71), eluted in three separate fractions, and dried using a vacuum concentrator.

LC-MS/MS data acquisition. Peptides were resuspended in 2% (v/v) acetonitrile and 0.1% (v/v) TFA. Aceylome, proteome and HDAC pulldown samples were measured using an EASY-nLC 1200 system coupled to an Exploris 480 mass spectrometer (Thermo Fisher Scientific). Myc pulldown and corresponding input samples were measured using an EASY-nLC 1200 system coupled to an Q Exactive HF mass spectrometer (Thermo Fisher Scientific). The peptides were separated on 20 cm fritless silica emitters with a 0.75 µm inner diameter (CoAnn). Emitters were packed in-house with reversed-phase 1.9 µm ReproSil-Pur C_{18}-AQ (Dr Maisch GmbH). A 115 min (78 min for Myc pulldown) LC gradient using 0.1% (v/v) formic acid as buffer A and 80% (v/v) acetonitrile, 0.1% (v/v) formic acid as buffer B was used. Data acquisition settings for all experiments are listed in *SI Appendix*, Table S7.

Acknowledgments

The authors are grateful to Ms. S. Nakae, Ms. K. Kaneko, and Ms. F. Sakai in the support unit for Bio-Material Analysis and RIKEN CBS Research Resources Division for technical help with the nucleotide sequencing analyses. We also thank Prof. M. Matsui and Dr. W.D. Ong at RIKEN for providing the *lea7-1* as well as Ms. A. Sato (Plant Genomic Network Research Team), Ms. T. Kaizuka (Drug Discovery Seeds Development Unit), Dr. K. Matsumoto (Drug Discovery Seeds Development Unit), Dr. A. Idei (Drug Discovery Seeds Development Unit) for technical support. We would like to thank Mrs. Paulina Heinkow for technical support with the LC-MS/MS analysis within the MSPUB proteomics unit of the University of Muenster. This work was supported by the following grants and funding agencies: ASPIRE JPMJAP24A3 (MS), CREST JPMJCR13B4 (MS), GteX programs of the Japan Science and Technology Agency JPMJGX23B0 (MS), “Epigenome Manipulation Project” and “Global Commons Project” of RIKEN (MS), the Ministry of Education Culture, Sports and Technology of Japan KAKENHI Grant 19K05960 (MU), and the Deutsche Forschungsgemeinschaft (DFG, German Research Foundation) – INST 211/744-1 FUGG for instrumentation (IF).

References

1. Tian L & Chen ZJ (2001) Blocking histone deacetylation in *Arabidopsis* induces pleiotropic effects on plant gene regulation and development. *Proc Natl Acad Sci U S A* 98(1):200-205.
2. Le H, Simmons CH, & Zhong X (2025) Functions and mechanisms of histone modifications in plants. *Annu Rev Plant Biol* 76(1):551-578.
3. Ueda M & Seki M (2020) Histone modifications form epigenetic regulatory networks to regulate abiotic stress response. *Plant Physiol* 182(1):15-26.
4. Long JA, Ohno C, Smith ZR, & Meyerowitz EM (2006) TOPLESS regulates apical embryonic fate in *Arabidopsis*. *Science* 312(5779):1520-1523.

5. Talbert PB & Henikoff S (2010) Histone variants-ancient wrap artists of the epigenome. *Nat Rev Mol Cell Biol* 11(4):264-275.
6. Kouzarides T (2007) Chromatin modifications and their function. *Cell* 128(4):693-705.
7. Strahl BD & Allis CD (2000) The language of covalent histone modifications. *Nature* 403(6765):41-45.
8. Jenuwein T & Allis CD (2001) Translating the histone code. *Science* 293(5532):1074-1080.
9. Allfrey VG, Faulkner R, & Mirsky AE (1964) Acetylation and methylation of histones and their possible role in the regulation of rna synthesis. *Proc Natl Acad Sci U S A* 51(5):786-794.
10. Penke TJR, McKay DJ, Strahl BD, Matera AG, & Duronio RJ (2018) Functional redundancy of variant and canonical histone H3 lysine 9 modification in *Drosophila*. *Genetics* 208(1):229-244.
11. Shahbazian MD & Grunstein M (2007) Functions of site-specific histone acetylation and deacetylation. *Annu Rev Biochem* 76:75-100.
12. Wollmann H*, et al.* (2012) Dynamic deposition of histone variant H3.3 accompanies developmental remodeling of the *Arabidopsis* transcriptome. *PLoS Genet* 8(5):e1002658.
13. Hollender C & Liu Z (2008) Histone deacetylase genes in *Arabidopsis* development. *J Integr Plant Biol* 50(7):875-885.
14. Mehdi S*, et al.* (2016) The WD40 domain protein MSI1 functions in a histone deacetylase complex to fine-tune abscisic acid signaling. *Plant Cell* 28(1):42-54.
15. Ueda M*, et al.* (2018) Versatility of HDA19-deficiency in increasing the tolerance of Arabidopsis to different environmental stresses. *Plant Signal Behav* 13(8):e1475808.
16. Ueda M*, et al.* (2017) The distinct roles of class I and II RPD3-like histone deacetylases in salinity stress response. *Plant Physiol* 175(4):1760-1773.
17. Wu Y*, et al.* (2025) OsHDAC1 deacetylates the aldehyde dehydrogenase OsALDH2B1, repressing *OsGR3* and decreasing salt tolerance in rice. *Plant Physiol* 198(1).
18. Luo M, Cheng K, Xu Y, Yang S, & Wu K (2017) Plant responses to abiotic stress regulated by histone deacetylases. *Front Plant Sci* 8:2147.
19. Hartl M*, et al.* (2017) Lysine acetylome profiling uncovers novel histone deacetylase substrate proteins in Arabidopsis. *Mol Syst Biol* 13(10):949.
20. Scholz C*, et al.* (2015) Acetylation site specificities of lysine deacetylase inhibitors in human cells. *Nat Biotechnol* 33(4):415-423.
21. Nunez-Vazquez R, Desvoyes B, & Gutierrez C (2022) Histone variants and modifications during abiotic stress response. *Front Plant Sci* 13:984702.
22. Liu N*, et al.* (2025) Essential angiosperm-specific subunits of HDA19 histone deacetylase complexes in Arabidopsis. *EMBO J* 44(12):3521-3546.
23. Dose A*, et al.* (2016) Interrogating substrate selectivity and composition of endogenous histone deacetylase complexes with chemical probes. *Angew Chem Int Edit* 55(3):1192-1195.
24. Probst AV, Desvoyes B, & Gutierrez C (2020) Similar yet critically different: the distribution, dynamics and function of histone variants. *J Exp Bot* 71(17):5191-5204.
25. Stroud H*, et al.* (2012) Genome-wide analysis of histone H3.1 and H3.3 variants in *Arabidopsis thaliana*. *Proc Natl Acad Sci U S A* 109(14):5370-5375.
26. Zhao T*, et al.* (2022) Histone H3.3 deposition in seed is essential for the post-embryonic developmental competence in Arabidopsis. *Nat Commun* 13(1):7728.
27. Tanaka M, Kikuchi A, & Kamada H (2008) The Arabidopsis histone deacetylases HDA6 and HDA19 contribute to the repression of embryonic properties after germination. *Plant Physiol* 146(1):149-161.
28. Tilak P*, et al.* (2023) Proteome-wide lysine acetylation profiling to investigate the involvement of histone deacetylase HDA5 in the salt stress response of Arabidopsis leaves. *Plant J* 115(1):275-292.

29. Hecht A, Laroche T, Strahl-Bolsinger S, Gasser SM, & Grunstein M (1995) Histone H3 and H4 N-termini interact with SIR3 and SIR4 proteins: a molecular model for the formation of heterochromatin in yeast. *Cell* 80(4):583-592.
30. Feng C*, et al.* (2021) Arabidopsis RPD3-like histone deacetylases form multiple complexes involved in stress response. *J Genet Genomics* 48(5):369-383.
31. Wang Z*, et al.* (2013) *Arabidopsis* paired amphipathic helix proteins SNL1 and SNL2 redundantly regulate primary seed dormancy via abscisic acid-ethylene antagonism mediated by histone deacetylation. *Plant Cell* 25(1):149-166.
32. Perrella G*, et al.* (2013) Histone deacetylase complex1 expression level titrates plant growth and abscisic acid sensitivity in *Arabidopsis*. *Plant Cell* 25(9):3491-3505.
33. de Boor S*, et al.* (2015) Small GTP-binding protein Ran is regulated by posttranslational lysine acetylation. *Proc Natl Acad Sci U S A* 112(28):E3679-3688.
34. Backues SK, Korasick DA, Heese A, & Bednarek SY (2010) The *Arabidopsis* dynamin-related protein2 family is essential for gametophyte development. *Plant Cell* 22(10):3218-3231.
35. Smith JM*, et al.* (2014) Loss of *Arabidopsis thaliana* Dynamin-Related Protein 2B reveals separation of innate immune signaling pathways. *PLoS Pathog* 10(12):e1004578.
36. Hundertmark M & Hincha DK (2008) LEA (late embryogenesis abundant) proteins and their encoding genes in *Arabidopsis thaliana*. *BMC Genomics* 9:118.
37. Zhao PS*, et al.* (2011) Overexpression of *AtLEA3-3* confers resistance to cold stress in *Escherichia coli* and provides enhanced osmotic stress tolerance and ABA sensitivity in *Arabidopsis thaliana*. *Mol Biol*+ 45(5):785-796.
38. Lang V & Palva ET (1992) The expression of a *rab*-related gene, *rab18,* is induced by abscisic acid during the cold acclimation process of *Arabidopsis thaliana* (L.) Heynh. *Plant Mol Biol* 20(5):951-962.
39. Zhou MM & Cole PA (2025) Targeting lysine acetylation readers and writers. *Nat Rev Drug Discov* 24(2):112-133.
40. Seto E & Yoshida M (2014) Erasers of histone acetylation: the histone deacetylase enzymes. *Cold Spring Harb Perspect Biol* 6(4):a018713.
41. Chen C*, et al.* (2017) Cytosolic acetyl-CoA promotes histone acetylation predominantly at H3K27 in *Arabidopsis*. *Nat Plants* 3(10):814-824.
42. Mahrez W*, et al.* (2016) H3K36ac Is an evolutionary conserved plant histone modification that marks active genes. *Plant Physiol* 170(3):1566-1577.
43. Benhamed M, Bertrand C, Servet C, & Zhou DX (2006) *Arabidopsis GCN5*, *HD1*, and *TAF1*/*HAF2* interact to regulate histone acetylation required for light-responsive gene expression. *Plant Cell* 18(11):2893-2903.
44. Saharan K, Baral S, Shaikh NH, & Vasudevan D (2024) Structure-function analyses reveal *Arabidopsis thaliana* HDA7 to be an inactive histone deacetylase. *Curr Res Struct Biol* 7:100136.
45. Zeng X*, et al.* (2020) HISTONE DEACETYLASE 9 functions with Polycomb silencing to repress *FLOWERING LOCUS C* Expression. *Plant Physiol* 182(1):555-565.
46. Perrella G*, et al.* (2024) Histone Deacetylase Complex 1 and histone 1 epigenetically moderate stress responsiveness of *Arabidopsis thaliana* seedlings. *New Phytol* 241(1):166-179.
47. Fong PM, Tian L, & Chen ZJ (2006) *Arabidopsis thaliana* histone deacetylase 1 (AtHD1) is localized in euchromatic regions and demonstrates histone deacetylase activity *in vitro*. *Cell Res* 16(5):479-488.
48. Varotto S*, et al.* (2003) Expression profile and cellular localization of maize Rpd3-type histone deacetylases during plant development. *Plant Physiol* 133(2):606-617.
49. Chen X*, et al.* (2016) POWERDRESS interacts with HISTONE DEACETYLASE 9 to promote aging in *Arabidopsis*. *Elife* 5.
50. Yang WM, Tsai SC, Wen YD, Fejer G, & Seto E (2002) Functional domains of histone deacetylase-3. *J Biol Chem* 277(11):9447-9454.

551 51. Kahali S, Sarcar B, Prabhu A, Seto E, & Chinnaiyan P (2012) Class I histone
552 deacetylases localize to the endoplasmic reticulum and modulate the unfolded protein
553 response. *FASEB J* 26(6):2437-2445.
554 52. Dure L, 3rd, Greenway SC, & Galau GA (1981) Developmental biochemistry of
555 cottonseed embryogenesis and germination: changing messenger ribonucleic acid
556 populations as shown by in vitro and in vivo protein synthesis. *Biochemistry* 20(14):4162-
557 4168.
558 53. Galau GA, Hughes DW, & Dure L, 3rd (1986) Abscisic acid induction of cloned cotton late
559 embryogenesis-abundant (*Lea*) mRNAs. *Plant Mol Biol* 7(3):155-170.
560 54. Browne J, Tunnacliffe A, & Burnell A (2002) Anhydrobiosis: plant desiccation gene found
561 in a nematode. *Nature* 416(6876):38.
562 55. Stacy RA & Aalen RB (1998) Identification of sequence homology between the internal
563 hydrophilic repeated motifs of group 1 late-embryogenesis-abundant proteins in plants
564 and hydrophilic repeats of the general stress protein GsiB of *Bacillus subtilis*. *Planta*
565 206(3):476-478.
566 56. Kovacs D, Kalmar E, Torok Z, & Tompa P (2008) Chaperone activity of ERD10 and
567 ERD14, two disordered stress-related plant proteins. *Plant Physiol* 147(1):381-390.
568 57. Koag MC, Fenton RD, Wilkens S, & Close TJ (2003) The binding of maize DHN1 to lipid
569 vesicles. Gain of structure and lipid specificity. *Plant Physiol* 131(1):309-316.
570 58. Chakrabortee S*, et al.* (2012) Intrinsically disordered proteins as molecular shields. *Mol*
571 *Biosyst* 8(1):210-219.
572 59. Knox-Brown P*, et al.* (2020) Similar yet different-structural and functional diversity among
573 *Arabidopsis thaliana* LEA_4 proteins. *Int J Mol Sci* 21(8).
574 60. Popova AV, Hundertmark M, Seckler R, & Hincha DK (2011) Structural transitions in the
575 intrinsically disordered plant dehydration stress protein LEA7 upon drying are modulated
576 by the presence of membranes. *Biochim Biophys Acta* 1808(7):1879-1887.
577 61. Ginsawaeng O*, et al.* (2021) Subcellular localization of seed-expressed LEA_4 proteins
578 reveals liquid-liquid phase separation for LEA9 and for LEA48 homo- and LEA42-LEA48
579 heterodimers. *Biomolecules* 11(12).
580 62. Popova AV, Rausch S, Hundertmark M, Gibon Y, & Hincha DK (2015) The intrinsically
581 disordered protein LEA7 from *Arabidopsis thaliana* protects the isolated enzyme lactate
582 dehydrogenase and enzymes in a soluble leaf proteome during freezing and drying.
583 *Biochim Biophys Acta* 1854(10 Pt A):1517-1525.
584 63. Pedrosa AM, Martins Cde P, Goncalves LP, & Costa MG (2015) Late Embryogenesis
585 Abundant (LEA) constitutes a large and diverse family of proteins Involved in
586 development and abiotic stress responses in sweet orange (*Citrus sinensis* L. Osb.).
587 *PLoS One* 10(12):e0145785.
588 64. Kamarudin ZS*, et al.* (2019) LEA gene expression assessment in advanced mutant rice
589 genotypes under drought stress. *Int J Genomics* 2019:8406036.
590 65. Wang X, Hu Y, Dong Y, Zhang L, & Wang B (2025) Abiotic stress-regulated *LEA* gene
591 mediates the response to drought, salinity, and cold stress in *Medicago sativa* L. *Plant*
592 *Cell Physiol* 66(5):781-796.
593 66. Kim KC, Lai Z, Fan B, & Chen Z (2008) *Arabidopsis* WRKY38 and WRKY62 transcription
594 factors interact with histone deacetylase 19 in basal defense. *Plant Cell* 20(9):2357-2371.
595 67. Liu K*, et al.* (2024) Histone variant H3.3 controls *Arabidopsis* fertility by regulating male
596 gamete development. *Plant Cell Physiol* 65(1):68-78.
597 68. Ong WD, Makita Y, Miyazaki T, Matsui M, & Shin R (2024) *Arabidopsis* transcriptomic
598 analysis reveals cesium inhibition of root growth involves abscisic acid signaling. *Planta*
599 259(2):36.
600 69. Rappsilber J, Mann M, & Ishihama Y (2007) Protocol for micro-purification, enrichment,
601 pre-fractionation and storage of peptides for proteomics using StageTips. *Nat Protoc*
602 2(8):1896-1906.
603 70. Wisniewski JR, Zougman A, Nagaraj N, & Mann M (2009) Universal sample preparation
604 method for proteome analysis. *Nat Methods* 6(5):359-362.

605 71. Lassowskat I*, et al.* (2017) Dimethyl-labeling-based quantification of the lysine acetylome
606 and proteome of plants. *Methods Mol Biol* 1653:65-81.
607 72. Hughes CS*, et al.* (2019) Single-pot, solid-phase-enhanced sample preparation for
608 proteomics experiments. *Nat Protoc* 14(1):68-85.
609 73. Zecha J*, et al.* (2019) TMT labeling for the masses: A robust and cost-efficient, in-solution
610 labeling approach. *Mol Cell Proteomics* 18(7):1468-1478.
611 74. Ritchie ME*, et al.* (2015) *limma* powers differential expression analyses for RNA-
612 sequencing and microarray studies. *Nucleic Acids Res* 43(7):e47.
613 75. Hooper C*, et al.* (2022) Subcellular Localisation database for Arabidopsis proteins
614 version 5.
615

616 **Figures**

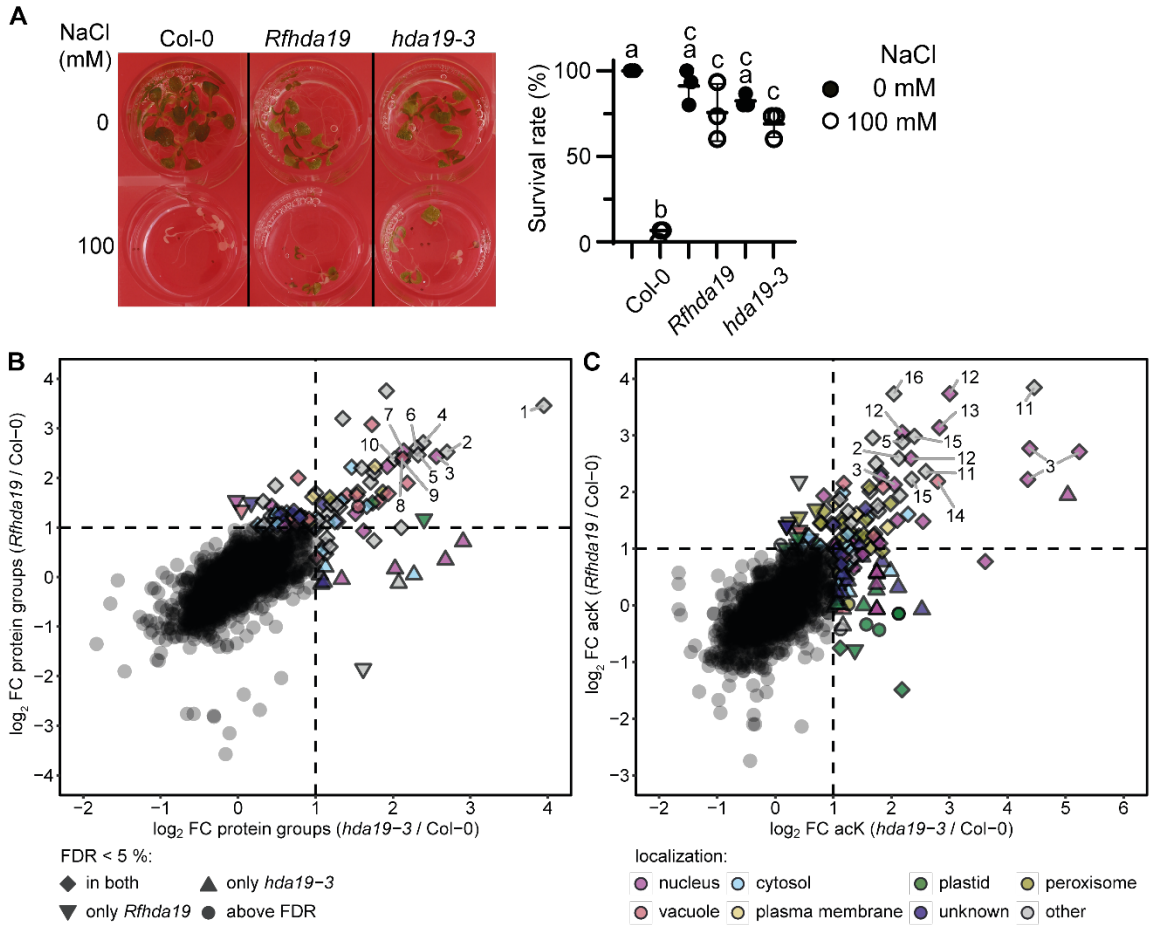

617
618 **Figure 1.** Identification of lysine-acetylated HDA19 substrates involved in plant stress tolerance.
619 (*A*) *Rfhda19*, a revertant in fertility of the *hda19-7* mutant, exhibited similar tolerance to salinity
620 stress (100 mM NaCl) as *hda19-3*. Multiple comparisons of survival rate were performed using one-
621 way ANOVA, with $P < 0.05$ considered significant (n=3). Inside diameter of the well is 15.4 mm. (*B*
622 and *C*) Scatter plots comparing (*B*) protein groups and (*C*) lysine acetylation (acK) site abundance
623 changes in *hda19-3* vs WT and *Rfhda19* vs WT. The original data can be found in Dataset S2 and
624 S3. Protein names or symbols of numbered spots are displayed in *SI Appendix*, Table S1.
625

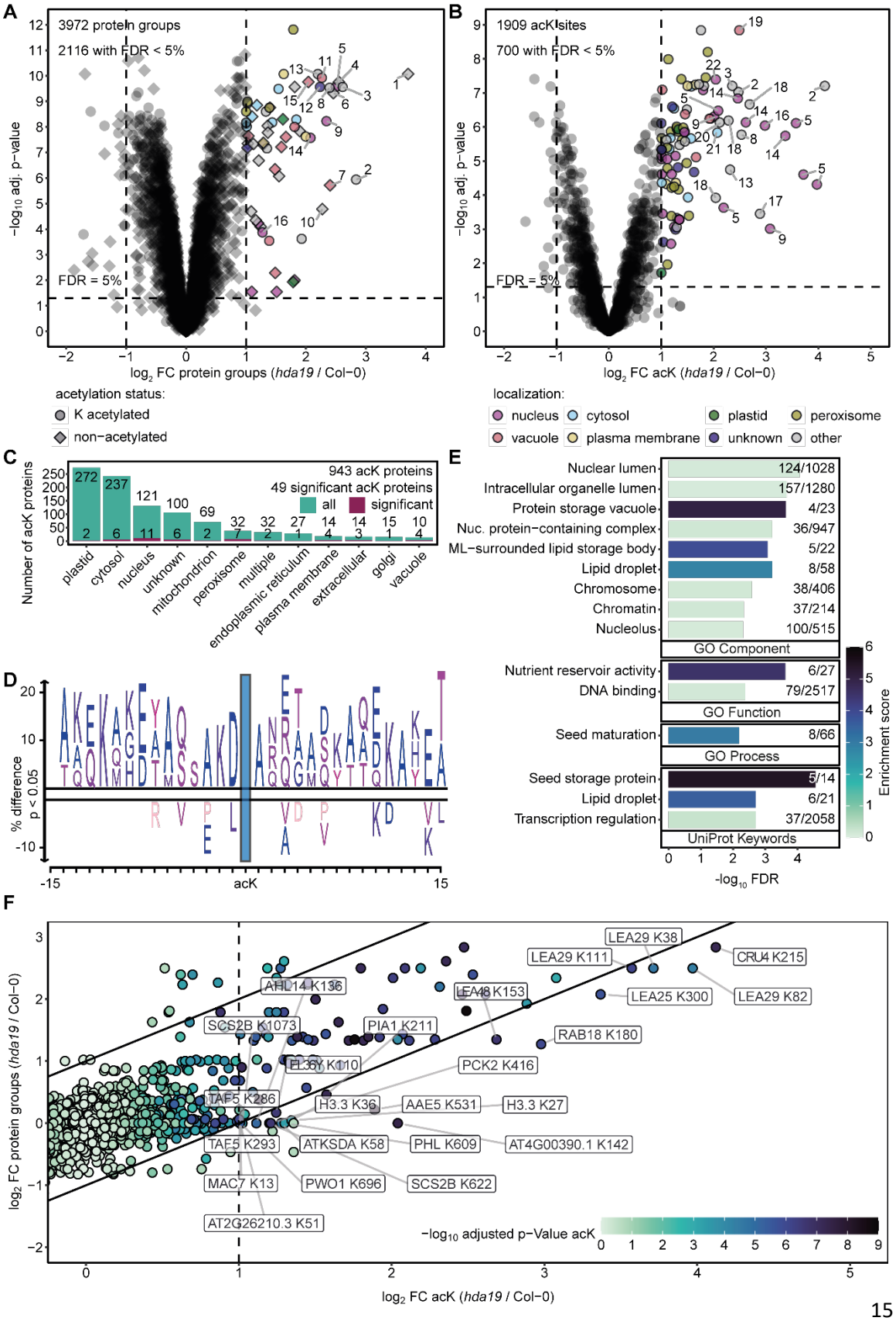
A
3972 protein groups
2116 with FDR < 5%
FDR = 5%
−log10 adj. p−value
log2 FC protein groups (hda19 / Col−0)
acetylation status:
K acetylated
non−acetylated
B
1909 acK sites
700 with FDR < 5%
FDR = 5%
−log10 adj. p−value
log2 FC acK (hda19 / Col−0)
localization:
nucleus
cytosol
plastid
peroxisome
vacuole
plasma membrane
unknown
other
C
943 acK proteins
49 significant acK proteins
all
significant
Number of acK proteins
plastid
cytosol
nucleus
unknown
mitochondrion
peroxisome
multiple
endoplasmic reticulum
plasma membrane
extracellular
golgi
vacuole
D
% difference
p < 0.05
acK
E
Nuclear lumen 124/1028
Intracellular organelle lumen 157/1280
Protein storage vacuole 4/23
Nuc. protein−containing complex 36/947
ML−surrounded lipid storage body 5/22
Lipid droplet 8/58
Chromosome 38/406
Chromatin 37/214
Nucleolus 100/515
GO Component
Nutrient reservoir activity 6/27
DNA binding 79/2517
GO Function
Seed maturation 8/66
GO Process
Seed storage protein 5/14
Lipid droplet 6/21
Transcription regulation 37/2058
UniProt Keywords
-log10 FDR
Enrichment score
F
LEA29 K38
LEA29 K111
CRU4 K215
AHL14 K136
LEA48 K153
LEA25 K300
LEA29 K82
SCS2B K1073
PIA1 K211
RAB18 K180
EL36Y K110
PCK2 K416
TAF5 K286
H3.3 K36
AAE5 K531
H3.3 K27
TAF5 K293
ATKSDA K58
PHL K609
AT4G00390.1 K142
MAC7 K13
PWO1 K696
SCS2B K622
AT2G26210.3 K51
−log10 adjusted p−Value acK
log2 FC protein groups (hda19 / Col−0)
log2 FC acK (hda19 / Col−0)

626

627 **Figure 2.** Identification of lysine-acetylated HDA19 substrates involved in plant stress tolerance. (*A*
628 and *B*) Volcano plots showing (*A*) protein groups and (*B*) lysine acetylation (acK) site log_2 fold
629 abundance changes in *hda19-3* compared to Col-0 WT, along with -log_{10}(adjusted p-values) from
630 *limma* analysis (74). The p-values were adjusted using a Benjamini-Hochberg correction. Data from
631 *hda19-3*, *Rfhda19* and WT were processed and analysed as one *hda19* group, and only acK sites
632 and protein groups quantified in at least 6 of 8 biological replicates were included in the analysis.
633 Log_2 fold changes (FC) of +/- 1 and false discovery rates (FDR) of < 5 % are indicated by dashed
634 lines. Significantly altered proteins and acK sites (log_2 FC > 1, FDR < 5 %) are colored according
635 to their SUBA5 localization (75). AcK sites and proteins with a log_2 FC > 2 are numbered. Protein
636 numbers with symbols or identifiers from 1 to 22: 1. AT2G05580, 2. CRU4, 3. CRU3, 4. PAP85, 5.
637 LEA29, 6. AT4G36700, 7. LEA18, 8. CRU1, 9. LEA7, 10. CRU2, 11. OLEO2, 12. OLEO4, 13.
638 LEA30, 14. LEA25, 15. CLO1, 16. RAB18, 17. SESA1, 18. LEA48, 19. OLEO1, 20. LEA42, 21.
639 LEA36, 22. AT4G00390. The original data is available in DataS4. (*C*) Subcellular localization of all
640 quantified acetylated proteins (green), and those which are significantly regulated in *hda19* vs WT
641 (purple) with a log_2 fold-change (FC) acK > 1, FDR < 0.05. (*D*) Sequence logo of significantly
642 upregulated acK sites in *hda19* (log_2 FC > 1, FDR < 0.05). The blue box indicates the position of
643 the acetylated lysine residue. (*E*) Functional enrichment analysis of all quantified acetylated
644 proteins in *hda19* vs WT. The bars represent the -log_{10}(FDR) for each term. The color of each bar
645 corresponds to the enrichment score for each term, calculated by STRING. The numbers adjacent
646 to the bars indicate the number of proteins found and the total number for each term. The analysis
647 included GO component, GO function, GO process, and UniProt keywords. Only terms showing an
648 increase in abundance are displayed. (*F*) Comparison of protein and acK log_2-fold changes in
649 *hda19* (*hda19-3* + *Rfhda19*). Nineteen proteins exhibited a significant increase in acetylation at 24
650 acK sites, exceeding their respective protein abundance changes. The lysine (K) positions of the
651 histone sites were adjusted to account for the removal of the initiator methionine. The original data
652 can be found in Dataset S4.

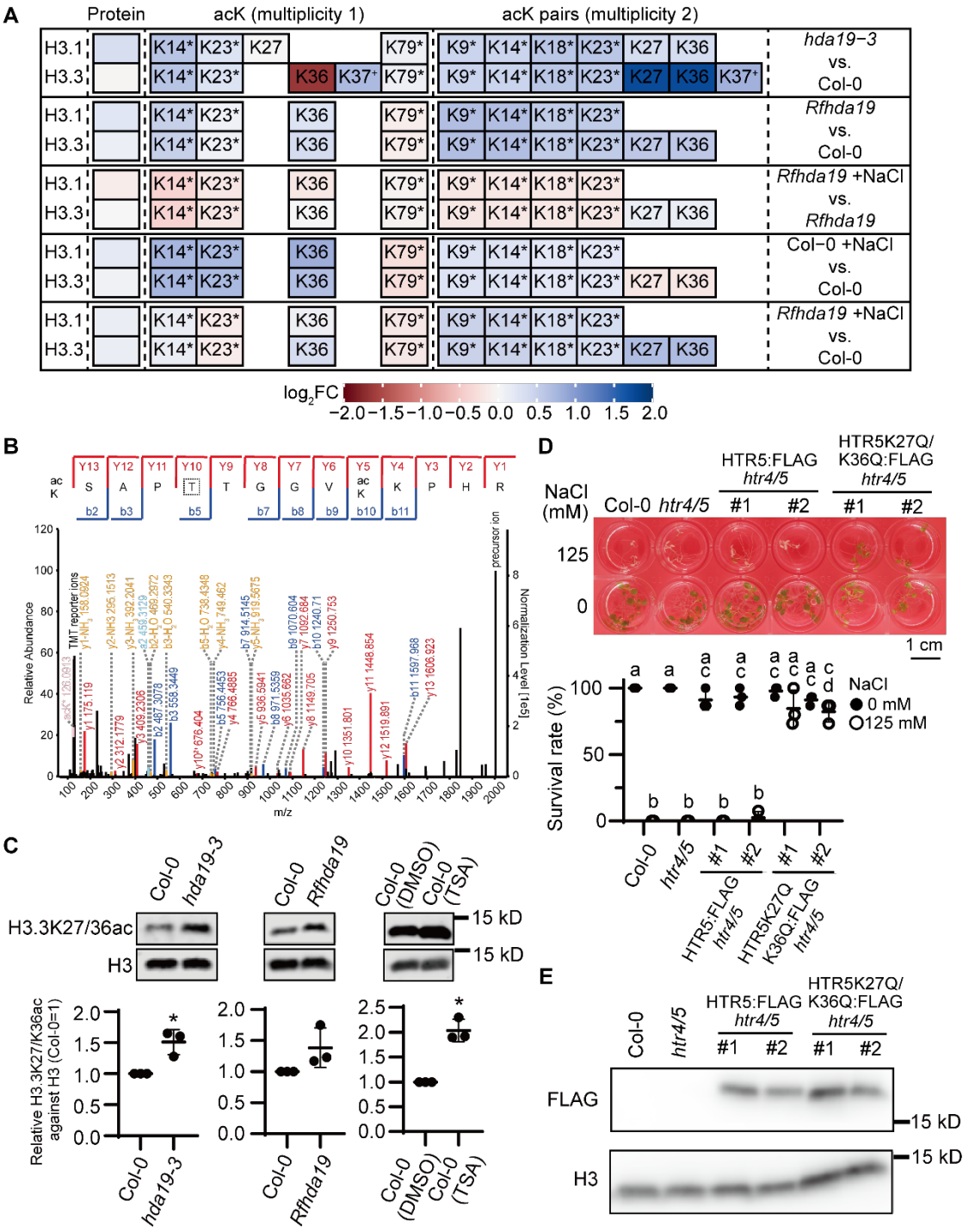

Figure 3. Requirement of H3.3K27/K36 di-acetylation for enhanced tolerance to salinity stress**.** (*A*) Protein and acK abundance of the two main histone 3 variants, H3.1 and H3.3, in *hda19-3*, *Rfhda19*, *Rfhda19* + NaCl, and WT + NaCl, were quantified in at least 2 out of 4 biological replicates. Colors indicate the respective $\log_2$ fold change (FC) values. Lysine positions have been adjusted to reflect the cleavage of the initiator methionine. The histone proteins can carry multiple acetylations and the number of distinct modified versions of the same peptide sequence that exist or are detected is therefore called multiplicity. Hence, lysine acetylation (acK) sites are grouped by

661 their respective multiplicity, as determined by MaxQuant. Stars next to the lysine (K) position
662 indicate sites that could belong to both histone variants. Di-acetylated (multiplicity 2) peptides of
663 H3.1 and H3.3 can be found in *SI Appendix*, Table S2. For acK sites marked with a +, we were not
664 able to clearly distinguish the modification sites K36 and K37 for all peptides, since these residues
665 are positioned next to each other in the peptide sequence. Distinctive fragment ions could be
666 identified to unambiguously localize K36ac, but not K37ac. The localization probability of K37ac is
667 around 0.5. (*B*) MS/MS spectra, as processed by MaxQuant, show an H3.3 peptide carrying K27
668 and K36 di-acetylation. The amino acid at position 31, which differentiates H3.3 from H3.1, is
669 marked by a dashed box. (*C*) Differences in histone H3 acetylation levels in the *hda19-3*, *Rfhda19*,
670 and plants treated with trichostatin A (TSA) were evaluated. Quantification of relative acetylation
671 levels was performed using Student's *t*-test (n=3, $P < 0.05$). (*D*) Expression of FLAG-tagged
672 HTR5K27Q/K36Q acetylation mimicking variant in *htr4/5* enhanced tolerance to salinity stress (125
673 mM NaCl). Multiple comparisons of survival rate were performed using one-way ANOVA, with $P <$
674 0.05 considered significant (n=3). (*E*) Immunoblotting of the FLAG-tagged HTR5 and FLAG-tagged
675 HTR5K27Q/K36Q is shown. The full blot is presented in *SI Appendix*, Fig. S1.

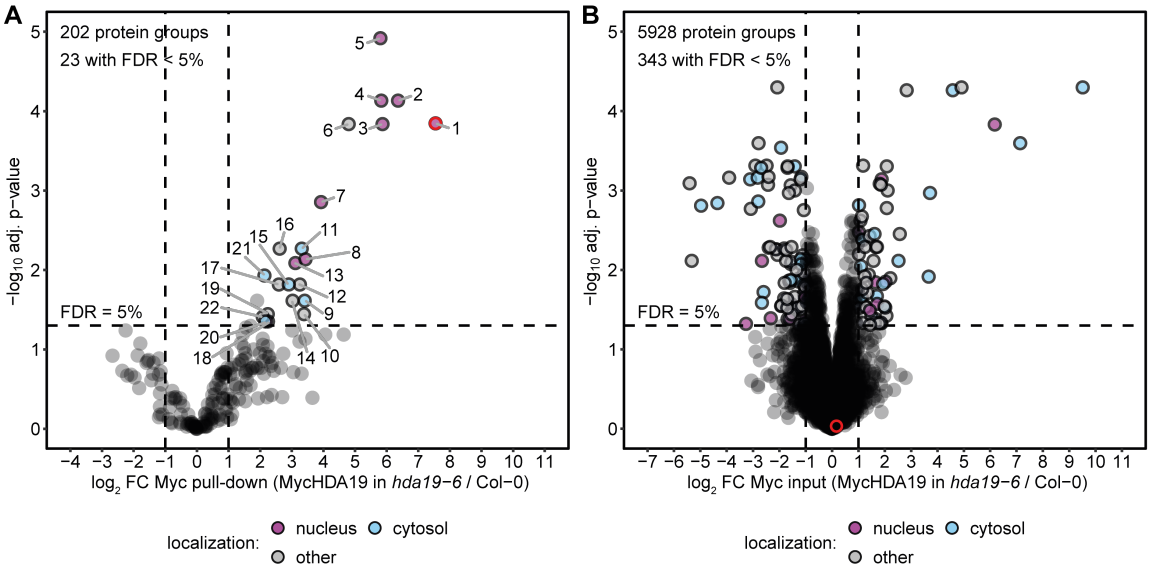

Figure 4. Identification of HDA19 interacting proteins. Volcano plots showing (*A*) enriched proteins in Myc pulldown and (*B*) overall protein abundance changes (input) in MycHDA19 (in *hda19-6*) compared to Col-0 WT, along with -$\log_{10}$(adjusted p-values) from *limma* analysis (74). The p-values were adjusted with Benjamini-Hochberg correction. Protein groups only quantified in at least 2 of 4 biological replicates were included in the analysis. Log_2 fold changes of +/- 1 and FDR of 5 % are indicated by dashed lines. Significantly enriched proteins ($\log_2$ FC > 1, FDR < 0.05) are colored according to their SUBA5 localization (75). Significantly enriched proteins with a $\log_2$ FC > 2 are numbered. Protein numbers with symbols or identifiers from 1 to 22: 1. HDA19, 2. HDC1, 3. ES25Y, 4. MSI1, 5. SNL5, 6. SNL4, 7. SNL6, 8. SNL2, 9. RPL5A, 10. AT5G36790, 11. CCT7, 12. HDIP3, 13. HB1, 14. FdC1, 15. RAN-1, 16. APOK3, 17. ICL, 18. SNL1, 19. CRU2, 20. RPS18C, 21. RPS26e, 22. LACS6. HDA19 is highlighted by a red circle in A and B. The original data can be found in Data S5.

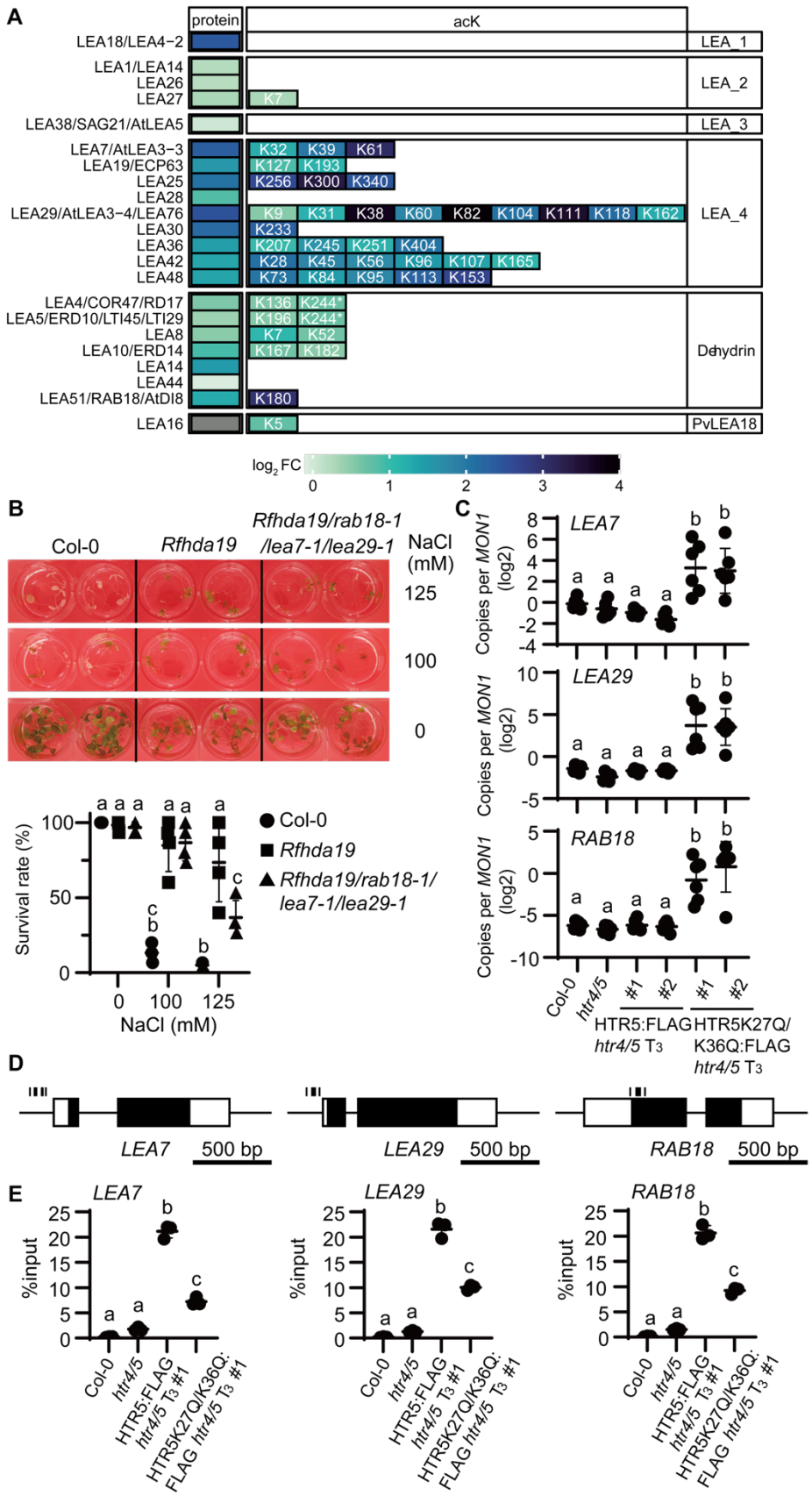
A
protein
acK
LEA18/LEA4−2
LEA_1
LEA1/LEA14
LEA26
LEA27
K7
LEA_2
LEA38/SAG21/AtLEA5
LEA_3
LEA7/AtLEA3−3
LEA19/ECP63
LEA25
LEA28
LEA29/AtLEA3−4/LEA76
LEA30
LEA36
LEA42
LEA48
K32 K39 K61
K127 K193
K256 K300 K340
K9 K31 K38 K60 K82 K104 K111 K118 K162
K233
K207 K245 K251 K404
K28 K45 K56 K96 K107 K165
K73 K84 K95 K113 K153
LEA_4
LEA4/COR47/RD17
LEA5/ERD10/LTI45/LTI29
LEA8
LEA10/ERD14
LEA14
LEA44
LEA51/RAB18/AtDI8
K136 K244*
K196 K244*
K7 K52
K167 K182
K180
Dehydrin
LEA16
K5
PvLEA18
log2 FC
0 1 2 3 4
B
Col-0
Rfhda19
Rfhda19/rab18-1 /lea7-1/lea29-1
NaCl (mM)
125
100
0
Survival rate (%)
NaCl (mM)
Col-0
Rfhda19
Rfhda19/rab18-1/ lea7-1/lea29-1
C
LEA7
LEA29
RAB18
Copies per MON1 (log2)
Col-0
htr4/5
#1
#2
HTR5:FLAG htr4/5 T3
HTR5K27Q/ K36Q:FLAG htr4/5 T3
D
LEA7
LEA29
RAB18
500 bp
E
%input
Col-0
htr4/5
HTR5:FLAG htr4/5 T3 #1
HTR5K27Q/K36Q: FLAG htr4/5 T3 #1

688

689 **Figure 5.** Identification of essential LEA proteins regulated by hyperacetylation of H3.3 for
690 enhancing salinity tolerance in *hda19* mutants. (*A*) Protein abundance and lysine acetylation site
691 (acK) levels of LEA proteins, quantified in at least 6 out of 8 replicates, are shown. The color
692 indicates the $\log_2$ fold change (FC) of *hda19* versus WT Col-0. Stars next to the K position indicate
693 sites that could belong to both LEA variants. (*B*) Deficiencies in three *LEA* genes
694 (*RAB18*/*LEA7*/*LEA29*) decreased tolerance to salinity stress in *Rfhda19* mutants under high salinity
695 stress conditions (125 mM NaCl). Statistical analysis was performed using a one-way ANOVA, with
696 $P < 0.05$ considered significant (n=4). (*C*) qPCR analysis of the mRNA expression of *LEA* genes in
697 FLAG-tagged fused HTR5 and HTR5K27Q/K36Q acetylation mimicking plants. The dataset was
698 normalized using the reference gene (*MON1*). Statistical analysis was performed using one-way
699 ANOVA, with $P < 0.05$ considered significant (n=6). Different letters indicate significant differences.
700 (*D*) Schematic diagrams of primers for ChIP-qPCR of *LEA7*, *LEA29*, and *RAB18* genes. White
701 boxes, black boxes, and dotted lines represent untranslated regions, exons, and amplified regions
702 by each primer pair, respectively. (*E*) ChIP assay for FLAG-tagged fused HTR5 and
703 HTR5K27Q/K36Q proteins using anti-FLAG antibody at the *LEA7*, *LEA29*, and *RAB18* genes.
704 Statistical analysis was performed using one-way ANOVA, with $P < 0.05$ considered significant
705 (n=3). Different letters indicate significant differences.

706

707

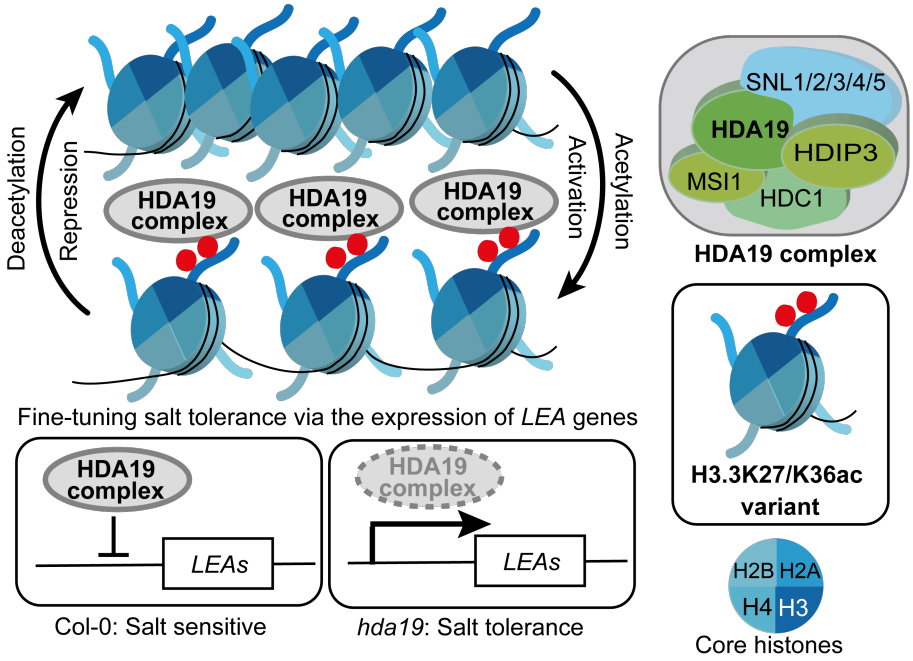

708 **Figure 6.** Schematic representation of a proposed mechanism of the response to salinity stress
709 regulated by HDA19. HDA19 complex regulates the expression of *LEA* genes (e. g.
710 *LEA7/LEA29/RAB18*) through di-acetylation of K27/K36 on histone H3.3.